Automating the Generation of Detailed Kinetic Models for Halocarbon Combustion with the Reaction Mechanism Generator

David S. Farina Jr., Sai Krishna Sirumalla, and Richard H. West*

Department of Chemical Engineering, Northeastern University, Boston, MA 02115, USA

E-mail: r.west@northeastern.edu

Abstract

Originally developed to predict the chemical kinetics of hydrocarbon combustion via automated generation of detailed reaction mechanisms, Reaction Mechanism Generator (RMG) contains extensive thermokinetic data for C,H,O chemisty, and has more recently been expanded to nitrogen and sulfur. In this work, we present the addition of halogen (fluorine, chlorine, and bromine) chemisty to RMG to enable automated generation of detailed kinetic models for halocarbon combustion. RMG's existing reaction templates are updated to include halogens, and 11 new reactions families are created specific to halogen chemistry. Notably, kinetics for more than 1000 elementary reactions are calculated via *ab inito* methods and transition state theory, and these kinetic data are combined with kinetics from literature sources to train rate rule decision tree estimators. Additionally, halogen groups are added to RMG's statistical mechanics database, enabling model generation with RMG's pressure dependence module and automated computation of microcanonical rate constants for unimolecular networks. Halogen groups are also incorporated in RMG's transport database to provide estimated parameters for the Lennard-Jones potential, important for transport-dependent

simulations including laminar flame speeds. To demonstrate RMG's capability for predicting halocarbon combustion, RMG is used to build a flame suppression model for 2-BTP (CH_2=$CBrCF_3$) in methane flames. The laminar flame speeds of RMG's 2-BTP model show good agreement with a published model under a variety of reaction conditions. Automating the generation of detailed kinetic models for halocarbon combustion will facilitate the exploration of previously unexplored reaction pathways, thereby accelerating the development of greener refrigerants and suppressants, as well as advancing the field of automated mechanism generation.

Introduction

Halocarbon Combustion

Halocarbons are widely used as refrigerant working fluids and flame suppressants. Chlorofluorocarbons (CFCs) and hydrochlorofluorocarbons (HCFCs) were among the first generation of these compounds, but were banned globally under the Montreal Protocol in the 1980s[1] due to their high ozone depletion potentials (ODPs). The second generation, mainly hydrofluorocarbons (HFCs), have low ODPs, but are currently being phased out due to their high global warming potentials (GWPs).[2] Despite these regulations on HFC production, a recent study found that HFC-23 (CHF_3) emissions reached an all-time high in 2018.[3]

The high GWPs of today's refrigerants and fire suppressants motivate the need for a third generation of environmentally-friendly halocarbon refrigerants and suppressants. However, the chemical properties that make potential replacement compounds greener also raise their flammability in very complicated ways.[4] For example, when used below their inerting concentration, many proposed fire suppressants (C_2HF_5, $C_6F_{12}O$, and CH_2=$CBrCF_3$) were found to *increase* overpressure, rather than decrease it in an FAA aerosol can test.[5]

The development of new and replacement of current compounds requires the rapid flammability screening of proposed compounds under different operating conditions. As the experimental study of all potential replacements is impractical, time-consuming, and costly, potential compounds are studied using flame simulations employing detailed kinetic mechanisms, supplemented by quantum chemistry calculations. In order to discover safe and effective replacements, mechanisms for current compounds, such as CF_3Br, have been thoroughly examined to gain a mechanistic understanding of what makes them effective at suppressing flames.[6] Understanding how current compounds work has led to potential candidates, such as 2-bromo-3,3,3-trifluoroprop-1-ene (2-BTP) (CH_2=$CBrCF_3$), that resemble current compounds but are more eco-friendly.

In recent years, 2-BTP has been heavily researched as a promising replacement for suppressant CF_3Br.[5,7] 2-BTP is of particular interest since it is a fluoro-alkene and has a shorter atmospheric lifetime due to the presence of a double bond, making it more eco-friendly than current suppressants.[8] Also, with a bromine atom and CF_3 group, it is predicted to have a similar fire-suppression performance to CF_3Br.[5] Through flame simulations based off the NIST HFC mechanism,[9] 2-BTP was found to decrease laminar flame speed for fuel-rich flames, but *increase* flame speeds for fuel-lean flames.[5,7] Since the combustion behavior of newly proposed compounds is quite complex, further research is needed to develop and understand their complex reaction mechanism and how they behave under different conditions. As these mechanisms are currently constructed by hand, progress is slow due to the vast number of pathways and unknown thermokinetic parameters that need to be considered. To expedite and advance this research, expanding automated mechanism generation to halocarbon combustion is a promising avenue for future development.

Reaction Mechanism Generation

In recent decades, detailed kinetic models have become ubiquitous in combustion research, enabling prediction of combustion properties that are difficult to determine experimen-

tally.[10,11] Predictive kinetic modeling of gas-phase hydrocarbon combustion is aided by automated kinetic model generation tools.[12] One such tool is Reaction Mechanism Generator (RMG), an open-source software package, written in Python, that automatically generates detailed kinetic models by proposing elementary reactions and predicting chemical properties (thermochemical, kinetic, transport, solvation, etc.) using a database of reaction templates, thermokinetic data, and estimation routines.[13,14]

Given user-defined initial species and conditions, RMG generates a model using a core-edge rate-based algorithm, by iteratively applying "reaction families" to generate all possible reactions among a set of "core" species, and evaluating the reaction flux to each core and "edge" species during a set of isothermal, isobaric simulations. If an edge species' flux exceeds a user-defined tolerance, the simulation is interrupted in order to move that species to the core, where it is reacted with other core species using the reaction families. The newly generated species are added to the edge, then RMG runs another simulation to determine if any more edge species with sufficient flux should be moved to the core. When no more edge species can be moved to the core for each user-specified simulation condition, the final model is contained within RMG's core.

Representing a particular reaction class, each reaction family has a recipe for mutating molecular graphs to create products from reactants, and has a depository of training reactions with kinetic parameters used to train the family's rate rules. The rate rules are arranged in a hierarchical decision tree, with the most general template at the trunk and increasingly specific templates descending each branch.

Molecules in RMG are represented as 2D graphs, with atoms as nodes and bonds as edges. Graph-theory methods are used to identify isomorphic structures and recognize functional groups when applying reaction family templates and estimating properties. During model generation, chemical properties for proposed species and reactions are first sought in libraries of known parameters, but are usually estimated on-the-fly using decision trees. Thermochemical parameters ($\Delta_f H^\circ_{298K}$, S°_{298K}, C_p^T) are typically estimated using Benson's

group additivity method[15] for closed-shell singlet species and the Hydrogen Bond Increment (HBI) scheme[16] for open-shell radicals. There are similar methods to estimate other properties, including solvation parameters, gas-phase transport parameters, and vibrational frequencies to calculate densities of state for pressure-dependence calculations.[13,14]

The success of RMG's rate-based algorithm in generating accurate kinetic models that capture the essential chemistry in complicated reactive systems depends on the generalizability of its reaction families and the accuracy of its thermokinetic parameters estimates. Originally developed to study the kinetics of hydrocarbon combustion, RMG contains many important reaction families for the pyrolysis and oxidation of hydrocarbon fuels, and its databases contain extensive, although not exhaustive, thermokinetic data for CHO chemistry. Since many short-lived intermediates and elementary reactions are difficult to isolate and determine experimentally, quantum chemistry methods are often used to calculate thermokinetic parameters. Recent progress on expanding RMG to model nitrogen,[17] sulfur,[18] and silicon[19] has shown that quantum chemistry calculations are a viable approach to expand RMG's databases and estimation methods to new chemical systems. The recent addition of extensive halocarbon thermochemistry to RMG, including seventeen thousand electronic structure calculations and new group additivity values, is documented in Farina et al.[20] This work describes RMG's expansion to halogen chemistry with the incorporation of halocarbon kinetics, as well as transport and pressure-dependence estimates. Adding halogens to RMG provides a much-needed flammability screening tool to facilitate the discovery and implementation of the next-generation of eco-friendly halocarbon refrigerants and flame suppressants.

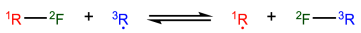

(a) F Abstraction

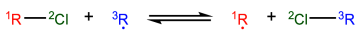

(b) Cl Abstraction

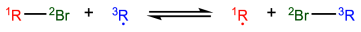

(c) Br Abstraction

(d) 1,2 XY Interchange

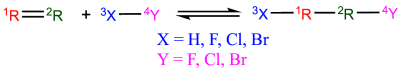

(e) XY Add MultipleBond

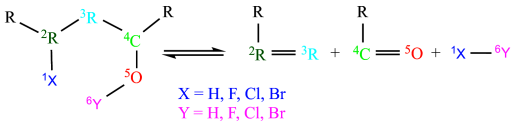

(f) XY Elim. Hydroxyl

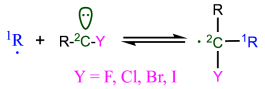

(g) Halocarbene Recombination

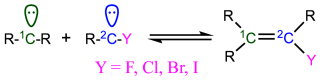

(h) Halocarbene Recombination Double

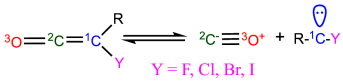

(i) Halocarbene CO Dimerization

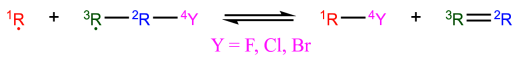

(j) Disproportionation-Y

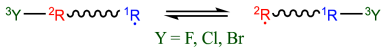

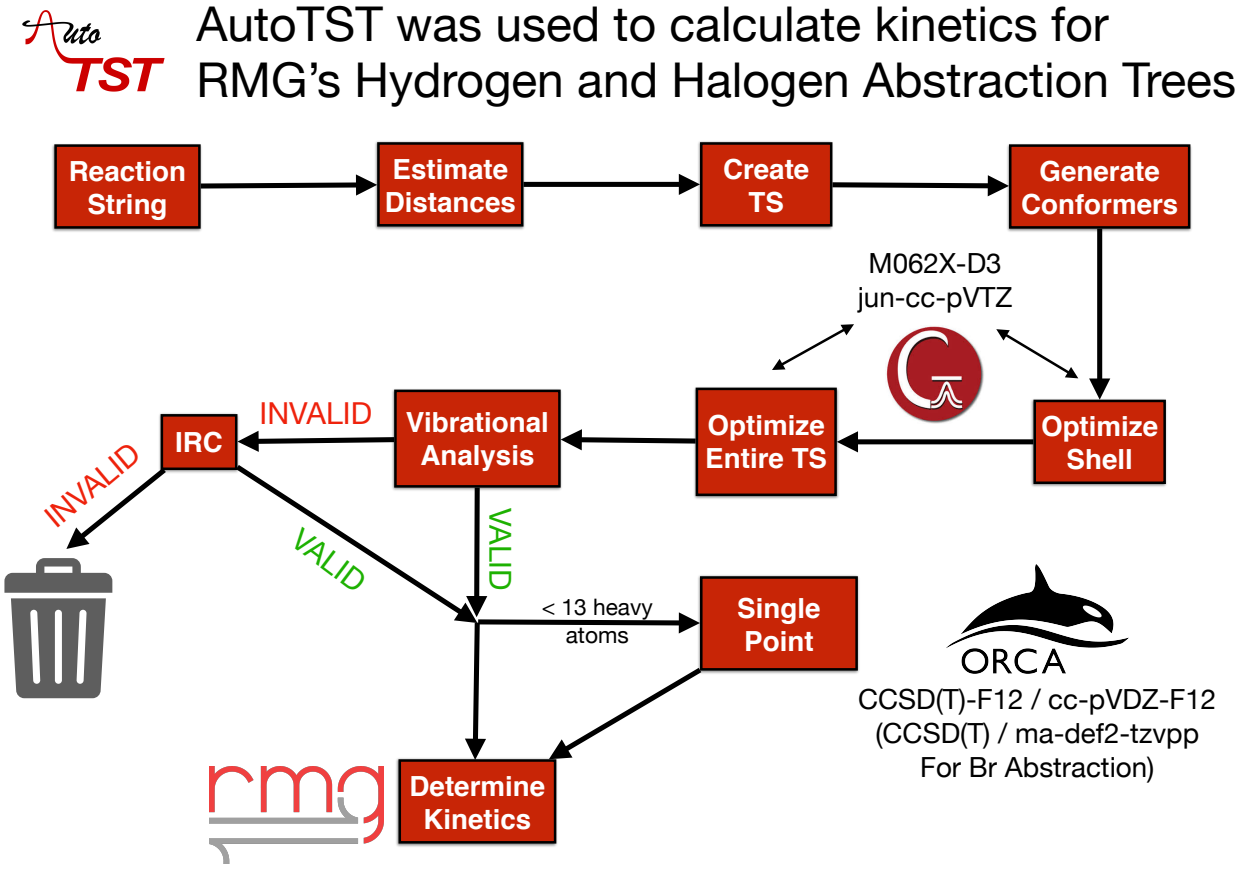

Figure 2: AutoTST workflow for optimizing transition states for abstraction reactions

Methods

New Reaction Families

To generate reactions with halogenated hydrocarbons, several of RMG's existing *default* reaction families such as H-abstraction and disproportionation were updated and 11 new reaction families, shown in Fig. 1, were created. Most of the families were created by examining reactions of halogenated species in literature mechanisms, and determining whether common reaction templates could be created to generate these reactions automatically. Other families were created based on suggested pathways in the literature and identifying transitions states in our own calculations. These new reaction families cover many essential pathways for halocarbon combustion including halogen abstractions (Fig. 1a-1c), halogen interchanges (1d), additions and eliminations (1e-1f), carbene chemistry (1g-1i), disproportionations (1j), and halogen migrations (1k). The halocarbene families were created to generate important reactions in halogen combustion such as the self-recombination of CF_2[21] and CCl_2[22] as well recombination reactions including carbenes such as CF_2 with radicals F, OH, and CH_3.[23]

To provide initial rate estimates for reactions generated with these new families, several halocarbon combustion mechanisms were imported into RMG from the literature, and reactions that matched a family template were added to the corresponding family's training reactions depository. Imported models include the NIST hydrofluorocarbon (HFC) mechanism[9,24] as well as kinetic models for CF_2BrCl,[25] 2-BTP and CF_3Br,[7] HFO-1234yf (CH_2=$CFCF_3$),[26] and CH_3Cl.[27]

The 1,2 XY Interchange family is based on the work of Kim et al.,[28] and RMG rate rules were created from their calculations. Several 1,1 and 1,2 HF/HCl/HBr eliminations from Brown et al.[29,30] and Smith et al.[31] were added as training to the 1,2 Insertion carbene and XY Addition Multiplebond families, respectively. Kinetics data from Yu et al.[32] and Srinivasan et al.[23] were added to the halocarbene recombination training set. The self-recombinations of CF_2[21] and CCl_2[22] were added as training data for the Halocarbene

recombination double family.

For several new families and default reaction families with new halogen kinetics training data, including hydrogen abstraction, decision trees were generated using RMG's automated tree generation algorithm.[14] Starting with the most general template at the root, the algorithm generates extensions based on the molecular graphs of the training reactions, chosen to maximize information gain at each level of the tree. For each node, a rate rule is created by fitting a Blowers Masel Arrhenius (ArrheniusBM) expression[33] to the training reactions' kinetics. During model generation, reaction rates are estimated by descending the tree as far as possible then using the enthalpy of reaction to evaluate the ArrheniusBM rate rule.

Since the rates for many reactions in the imported literature models are estimates, reaction family kinetic estimators trained on these data are sometimes quite inaccurate. Therefore, kinetics for all imported literature training reactions for halogen and hydrogen abstraction reactions were recalculated using AutoTST,[34,35] and the literature rates in the training set were replaced with calculated rates. To further improve rate rule estimates, sample reactions were generated at nodes with high uncertainties, and these reactions were calculated and added to the training set, and the trees regenerated. The predicted uncertainties at each node in the kinetics tree are calculated assuming a lognormal rate distribution at 1000 K. We sampled reactions at nodes with standard deviations in ln(k) greater than 3.

Automated Transition State Theory Calculations

The AutoTST workflow used to calculate kinetic parameters (A, n, and E_a) for halogen and hydrogen abstraction reactions is shown in Fig. 2.[34,35] First, a reaction string is used to generate an AutoTST Reaction object, and the reaction is matched to its RMG reaction family. Next, the key distances in the reaction center are estimated using AutoTST's database for the corresponding RMG reaction family. With these estimated distances, a "guess" of the transition state (TS) for the reaction is embedded with RDKit[36] to create a 3D geometry. After embedding, conformers are systematically explored using the algorithm implemented

in AutoTST,[34,35] which rotates dihedrals in 120° increments, alternates cis/trans isomerism of double bonds, and varies R/S stereochemistry for chiral centers (RMG does not currently track or preserve stereochemistry). Transition state conformers are minimized with the dftb+ calculator[37] and the halorg-0-1 parameter set[38] in ASE[39] while fixing the reaction center distances to keep the TS intact and avoid descending to the reactants or products. A unique set of low-energy transition state "guesses" is assembled (usually about 5–10) by discarding structurally similar molecules with a root-mean-square deviation below 0.1 Å of another TS in the set, then discarding TSs with electronic energies more than 5 kcal/mol above the lowest energy TS in the ensemble.

Each initial TS undergoes two DFT optimizations: a "shell" minimization where the reaction center distances are fixed, followed by a saddle point search of the entire TS. These optimizations are performed in Gaussian 16[40] using M06-2X-D3/jun-cc-pvtz (the M06-2X functional with Grimme's D3 empirical dispersion[41] and the jun-cc-pvtz basis set[42]) with the "UltraFine" pruned (99,590) grid. The M06-2X functional was chosen because it is accurate for barrier height calculations[43] and halocarbon geometries and energies.[44,45]

After all TSs have been optimized, the lowest energy TS is identified and AutoTST's vibrational analysis method is used to validate that the correct TS has been located. This method displaces the atoms in the TS using the negative frequency from the TS optimization. The TS is validated if the average change in the reaction center bonds is more than an order of magnitude greater than the average change in the "shell" bonds. If the TS can not be validated via vibrational analysis (about 1 time in 8), an intrinsic reaction coordinate (IRC) calculation is run in Gaussian 16 to determine if the TS connects the expected reactant and product structures. If the TS is still invalid, it is discarded, and the next lowest energy TS undergoes the validation procedure until a valid TS is found.

If a TS is validated and it has 12 or fewer heavy atoms, a more rigorous single-point calculation is performed in ORCA[46] to obtain more accurate barrier heights. Bromine abstractions are calculated with CCSD(T)/ma-def2-tzvpp (because there are no F12 basis sets

for Br), and CCSD(T)-F12/cc-pVDZ-F12 is used for all other abstraction reactions. Lastly, RMG's statistical mechanics calculator Arkane[47] is used to obtain elementary high pressure kinetics in modified Arrhenius form.

Reaction Mechanism Generation

To assess RMG's ability to generate detailed kinetic models for halocarbon combustion, RMG was used to construct a model for $C_3H_2F_3Br$ (2-BTP) and CF_3Br in methane flames. This model was built using the *Foundational Fuel Chemistry Model Version 1.0*[48] as a seed mechanism providing thermochemistry, reactions, and kinetics for small hydrocarbon combustion, and halogenated hydrocarbon thermochemistry libraries from Farina et al.[20] Reactions involving halogenated species were added from the reaction families described in this work. An RMG library of transport properties was created from the imported NIST mechanism, so for all of the halogen species the two models have in common, the NIST transport library was used. If a species is not in the library, the transport properties are estimated using RMG's algorithm[13] which uses critical properties estimated using Joback's Group Additivity method; the latter needed updating for halogenated hydrocarbons using the method of Devotta et al.[49] This, and the extended ability to estimate densities of states for pressure-dependent and fall-off reaction calculations, is detailed in the PhD dissertation by Farina.[50]

Flame Speed Simulations

The RMG 2-BTP model of 504 species and 9,515 reactions was compared to a literature mechanism[7] of 188 species and 1,610 reactions by calculating 1D laminar flame speeds in Cantera.[51] The flame speeds were evaluated at 300 K, 1 atm, and a wide range of methane/air equivalence ratios (ϕ = 0.5–1.2) and suppressant volume fractions (0 – 0.05). Since there is a large discrepancy in the uninhibited methane burning velocity between the two models,

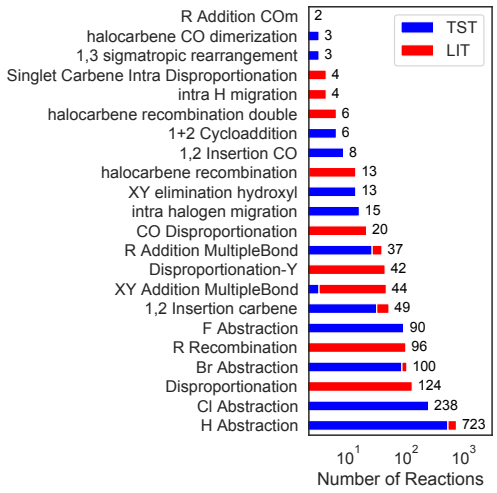

Figure 3: Number of halogen training reactions per reaction family. TST: calculated in this work, LIT: imported from literature

the normalized flame speeds were compared by dividing the velocity of the suppressed flame by the velocity of the uninhibited flame.

Local reaction sensitivity coefficients were computed by increasing the rate of each reaction i by 1%, one at a time, and calculating the percent change in the flame speed as follows:

$$s_i = \frac{Su_i - Su_0}{Su_0 \times 0.01} \tag{1}$$

where s_i is the sensitivity coefficient of reaction i, Su_i is the flame speed with reaction i accelerated by 1%, and Su_0 is the unperturbed base case flame speed. Sensitivities were computed for lean flames (equivalence ratio of 0.6 for 2-BTP and 0.7 for CF_3Br) and fuel rich flames (equivalence ratio of 1.2 for 2-BTP and CF_3Br). A suppressant volume fraction of 0.01 was used for all sensitivity computations.

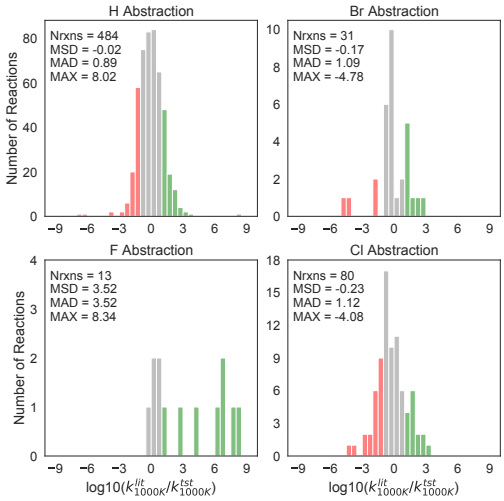

Figure 4: Comparison of AutoTST rate constants against literature rate constants for abstraction reactions at 1000 K. The literature often overestimates rates for fluorine abstractions. Green: Literature is $\geq$ 1 order of magnitude faster, Red: Literature is $\geq$ 1 order of magnitude slower.

Results

Kinetics Trees

Figure 3 shows the number of literature and calculated halogen training reactions for each RMG reaction family. Of the 1,640 training reactions, 1,031 were calculated in this work and 609 were added from the literature. Most of the calculated rates are for abstraction reactions (H, F, Cl, Br). Since AutoTST could not yet be used for other reactions families, non-abstraction rates were calculated "by hand" (using DFT and TST but with the initial geometries determined by a human) and added to training.

Figure 4 compares AutoTST calculated rates at 1000 K against literature rates for abstraction reactions. The majority of hydrogen abstraction reactions are within an order of magnitude and the mean absolute deviation (MAD) is close to 0; the literature models estimate these rates quite well. According to our TST calculations, fluorine abstraction reactions are relatively slow, and tend to be overestimated in literature models, sometimes by many orders of magnitude; this makes the decision-tree estimates too fast if the estimator

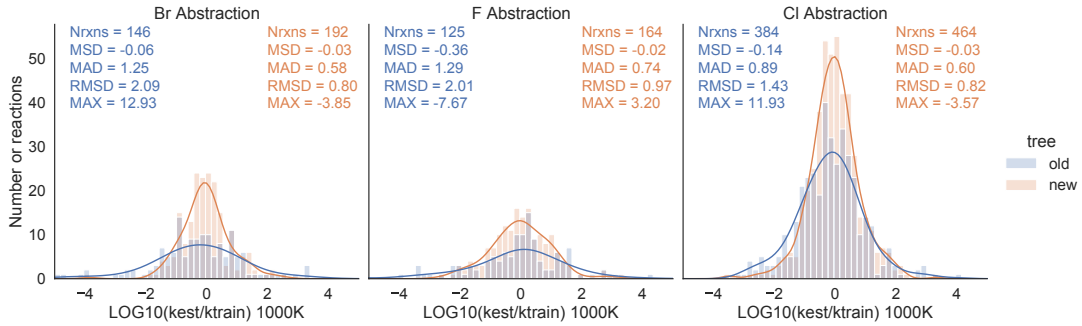

Figure 5: Cross-validation of halogen abstraction rate rule estimators before and after the addition of AutoTST calculated rates. The incorporation of more AutoTST calculated rates in training improves the rate rule estimates of halogen abstraction trees. old: Training set with literature rates, new: Training set with literature rates replaced with AutoTST rates

is trained on the literature values. The outliers, where a published rate is very different from our TST calculated rate, are mostly estimates. They may suffice in the context of the model they were published in, but they cause problems if estimation algorithms are trained on them for use elsewhere. For training estimators it is important to have accurate, robust, and consistent training data, i.e. calculated rates rather than estimates.

This is further demonstrated by the cross-validation results in Fig. 5. These plots show the predictive ability of the decision trees to estimate the rates of training reactions that have been excluded from the training set in a leave-one-out cross-validation procedure. The blue histograms ("old tree") show the predictions using training data comprising literature values supplemented with AutoTST rates for reactions sampled from uncertain nodes, where the mean absolute deviation was about an order of magnitude (0.89 for Cl abstraction, to 1.29 for F abstraction). The orange histograms ("new tree") show the improvement by recalculating the values previously taken from the literature and using only AutoTST rates as training data; the decision-tree estimators are better able to predict the missing data, with MAD errors between 0.58 (Br abstraction) and 0.74 (F abstraction) orders of magnitude. Under the assumption that the TST rates are correct, the decision tree estimators are thus performing better than current literature models (Fig. 4). These estimators can be further improved by adding calculated rates for reactions generated from nodes with a high uncertainty.

Flame Speed Simulations

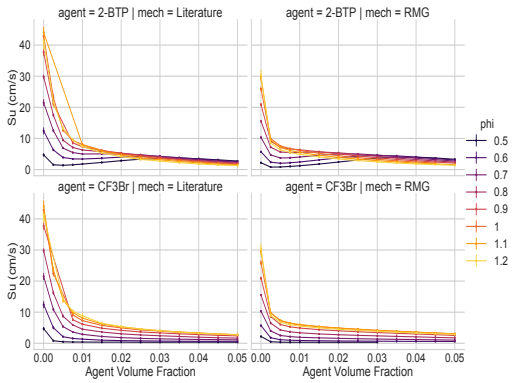

(a) Flame Speeds

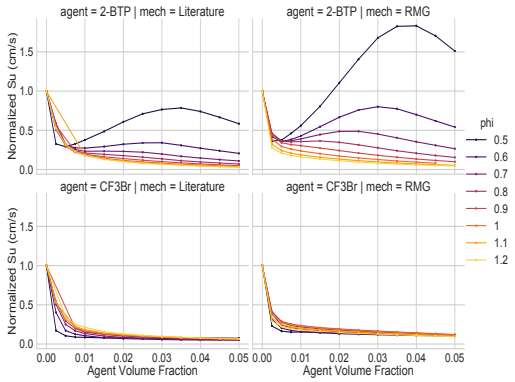

(b) Normalized Flame Speeds

Figure 6: Computed burning velocities of methane flames with added suppressant agents 2-BTP or CF_3Br for a literature mechanism[7] (mech = Literature) and an RMG mechanism (mech = RMG) as described in Section .

Figure 6 shows how the premixed methane/air laminar flame speeds change for the literature and RMG mechanisms when the suppressing agent (2-BTP or CF_3Br) is added. Although there is a large disagreement in the uninhibited methane burning velocities for the two models (a consequence of the seed mechanism chosen, not the halocarbon chemistry added in the current work), the RMG model shows remarkably good agreement with the literature mechanism at higher equivalence ratios (phi $\geq$ 0.7) over a wide range of suppressant volume fractions.

Figure 7 shows 18 of the top 20 most sensitive reactions for the RMG CF_3Br and 2-BTP

model under fuel rich and fuel lean conditions. For both suppressants, the 2 most sensitive reactions were excluded from the analysis because they are often very sensitive in hydrocarbon combustion mechanisms:

1. $H + O_2 \rightleftharpoons O + OH$
2. $CO + OH \rightleftharpoons CO_2 + H$

The sensitivity analysis reveals that RMG found many of these essential reaction pathways involving Br and HBr. The scavenging of H and OH radicals by HBr both have large negative sensitivities and inhibit combustion:

- $HBr + OH \longrightarrow Br + H_2O$
- $HBr + H \longrightarrow Br + H_2$

RMG also found important reactions that regenerate HBr which have negative sensitivities:

- $Br + HCO \longrightarrow HBr + CO$
- $Br + H \longrightarrow HBr$

Another important reaction pathway RMG found was the trapping of H atoms by CF_3, an inhibiting species in the CF_3Br and 2-BTP mechanisms.

- $CF_3 + H \longrightarrow CH_3F$

Importantly, RMG is able to automatically discover the important flame inhibition reactions involving halogens that scavenge reactive radicals such as H and OH, thereby suppressing flame propagation. Additionally, the RMG model is able to capture the "fuel effect" of 2-BTP, discussed in,[5] which enhances flame speeds for lean methane/air flames.

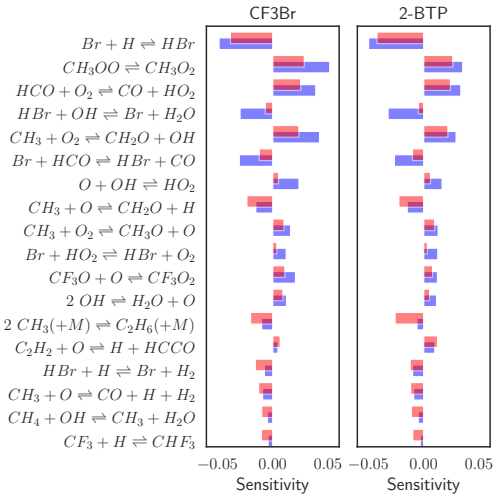

Figure 7: The most sensitive reactions in the RMG 2-BTP/CF_3Br mechanism for flame speeds of methane in air suppressed by 1% of the suppressant (CF_3Br left and 2-BTP (right). Sensitivities for the fuel lean conditions ($\phi = 0.6$ for 2-BTP and $\phi = 0.7$ for CF_3Br) is shown in blue, and fuel rich conditions is shown in red ($\phi = 1.2$).

Conclusions

Adding halogens to RMG will provide a much-needed flammability screening tool to facilitate the discovery and implementation of the next-generation of eco-friendly refrigerant fluids and fire suppressants. In this work, halogens are incorporated into RMG's existing reaction templates, and 11 new reactions families are created to automatically explore reaction pathways essential for halocarbon combustion. To obtain high fidelity reaction rate training data for decision tree rate rule estimators, kinetics from various literature sources are compiled, and more than 1000 elementary reactions are computed using *ab inito* quantum chemistry methods and transition state theory. Most hydrogen abstraction rates computed in this work show good agreement with literature rates. However, our calculations reveal a tendency for the literature to overestimate fluorine abstractions, and there are significant outliers for hydrogen and halogen abstractions which are often estimates in literature models. We also demonstrate how high-throughput calculation of halogen kinetics can improve the quality of reaction rate training data sets, thereby improving the predictions of decision tree rate estimators on unseen data.

To demonstrate RMG's new ability to generate halocarbon combustion models, RMG is used to build a 2-BTP kinetic model with 504 species and 9,515 reactions. Predicted methane/air flame speeds with added suppressant were in close agreement for the literature and RMG 2-BTP mechanisms, even though the RMG model has 316 more species and 7,905 more reactions. Thus, although flame speeds appear to be insensitive to these newly discovered species and reactions, a more thorough investigation into RMG's mechanism is necessary to determine if these intermediates and pathways are important to halocarbon flame suppression.

A significant contribution of this work, the ability to generate detailed kinetic models for the combustion of halogenated hydrocarbons with the fully automated Reaction Mechanism Generator (RMG) is an important breakthrough for combustion research. This work enables the investigation of novel halocarbon compounds, their interactions when blended, and their effects on different fuels. It is also a step towards modeling the incineration of per-and polyfluoroalkyl substances (PFAS), and the combustion of fluorinated liquid electrolytes in batteries.

Acknowledgement

This material is based upon work supported by the National Science Foundation under Grant No. 1751720. The authors acknowledge Information Technology Services, Research Computing at Northeastern University for providing high performance computing and storage, related software, visualization, and consulting resources. The authors thank Professor Bozzelli for sharing work on fluorine thermochemistry and GAVs, and also thank Dr. Linteris and Dr. Burgess for providing their HFC and 2-BTP/CF_3Br kinetic models. Sai Krishna Sirumalla acknowledges funding from Entos Inc through LEADERs program at Northeastern University.

Supporting Information Available

The training reactions and and estimation decision trees are publicly available in RMG's open-source database (`https://github.com/ReactionMechanismGenerator/RMG-database`) and also accessible through the *kinetics search* function on the RMG website (`https://rmg.mit.edu/database/kinetics/search/`). The data presented in this manuscript (and scripts to reproduce them) are all available at `https://doi.org/m9.figshare.20224851`.

References

(1) Montreal Protocol on Substances that Deplete the Ozone Layer Final Act 1987. *J. Environ. Law* **1989**, *1*, 128–136, DOI: 10.1093/jel/1.1.128.

(2) Harby, K. Hydrocarbons and their mixtures as alternatives to environmental unfriendly halogenated refrigerants: An updated overview. *Renew. Sust. Energ. Rev.* **2017**, *73*, 1247–1264, DOI: 10.1016/j.rser.2017.02.039.

(3) Stanley, K. M.; Say, D.; Mühle, J.; Harth, C. M.; Krummel, P. B.; Young, D.; O'Doherty, S. J.; Salameh, P. K.; Simmonds, P. G.; Weiss, R. F.; Prinn, R. G.; Fraser, P. J.; Rigby, M. Increase in global emissions of HFC-23 despite near-total expected reductions. *Nature Commun.* **2020**, *11*, 397, DOI: 10.1038/s41467-019-13899-4.

(4) Linteris, G.; Babushok, V. Numerically-Predicted Burning Velocities of C1 and C2 Hydrofluorocarbon Refrigerant Flames with Air. 17th International Refrigeration and Air Conditioning Conference at Purdue, West Lafayette, IN, 2018.

(5) Babushok, V. I.; Linteris, G. T.; Burgess, D. R.; Baker, P. T. Hydrocarbon flame inhibition by $C_3H_2F_3Br$ (2-BTP). *Combust. Flame* **2015**, *162*, 1104–1112, DOI: 10.1016/j.combustflame.2014.10.002.

(6) Westbrook, C. K. Numerical Modeling of Flame Inhibition by CF_3Br. *Combust. Sci. Technol.* **2007**, *34*, 201 – 225, DOI: 10.1080/00102208308923693.

(7) Burgess, D. R.; Babushok, V. I.; Linteris, G. T.; Manion, J. A. A Chemical Kinetic Mechanism for 2-Bromo-3,3,3-trifluoropropene (2-BTP) Flame Inhibition. *Int. J. Chem. Kinet.* **2015**, *47*, 533–563, DOI: 10.1002/kin.20923.

(8) Tapscott, R. E.; Mather, J. Tropodegradable fluorocarbon replacements for ozone-depleting and global-warming chemicals. *J. Fluorine Chem.* **2000**, *101*, 209–213, DOI: 10.1016/S0022-1139(99)00161-X.

(9) Burgess, D. R.; Zachariah, M. R.; Tsang, W.; Westmoreland, P. R. Thermochemical and chemical kinetic data for fluorinated hydrocarbons. *Prog. Energy Combust. Sci.* **1995**, *21*, 453–529, DOI: 10.1016/0360-1285(95)00009-7.

(10) Kohse-Höinghaus, K. Combustion in the future: The importance of chemistry. *Proc. Combust. Inst.* **2020**, *38*, 1–56, DOI: 10.1016/j.proci.2020.06.375.

(11) Miller, J. A.; Sivaramakrishnan, R.; Tao, Y.; Goldsmith, C. F.; Burke, M. P.; Jasper, A. W.; Hansen, N.; Labbe, N. J.; Glarborg, P.; Zádor, J. Combustion chemistry in the twenty-first century: Developing theory-informed chemical kinetics models. *Prog. Energy Combust. Sci.* **2021**, *83*, 100886, DOI: 10.1016/j.pecs.2020.100886.

(12) Vijver, R. V. d.; Vandewiele, N. M.; Bhoorasingh, P. L.; Slakman, B. L.; Khanshan, F. S.; Carstensen, H.-H.; Reyniers, M.-F.; Marin, G. B.; West, R. H.; Geem, K. M. V. Automatic Mechanism and Kinetic Model Generation for Gas- and Solution-Phase Processes: A Perspective on Best Practices, Recent Advances, and Future Challenges. *Int. J. Chem. Kinet.* **2015**, *47*, 199 – 231, DOI: 10.1002/kin.20902.

(13) Gao, C. W.; Allen, J. W.; Green, W. H.; West, R. H. Reaction Mechanism Generator: Automatic construction of chemical kinetic mechanisms. *Comput. Phys. Commun.* **2016**, *203*, 212–225, DOI: 10.1016/j.cpc.2016.02.013.

(14) Liu, M.; Grinberg Dana, A.; Johnson, M. S.; Goldman, M. J.; Jocher, A.; Payne, A. M.; Grambow, C. A.; Han, K.; Yee, N. W.; Mazeau, E. J.; Blondal, K.; West, R. H.; Goldsmith, C. F.; Green, W. H. Reaction Mechanism Generator v3.0: Advances in Automatic Mechanism Generation. *J. Chem. Inf. Model.* **2021**, *61*, 2686–2696, DOI: 10.1021/acs.jcim.0c01480.

(15) Benson, S. W.; Cruickshank, F. R.; Golden, D. M.; Haugen, G. R.; O'Neal, H. E.; Rodgers, A. S.; Shaw, R.; Walsh, R. Additivity rules for the estimation of thermochemical properties. *Chem. Rev.* **1969**, *69*, 279–324, DOI: 10.1021/cr60259a002.

(16) Lay, T. H.; Bozzelli, J. W.; Dean, A. M.; Ritter, E. R. Hydrogen Atom Bond Increments for Calculation of Thermodynamic Properties of Hydrocarbon Radical Species. *J. Phys. Chem.* **1995**, *99*, 14514–14527, DOI: 10.1021/j100039a045.

(17) Dana, A. G.; Buesser, B.; Merchant, S. S.; Green, W. H. Automated Reaction Mechanism Generation Including Nitrogen as a Heteroatom. *Int. J. Chem. Kinet.* **2018**, *50*, 243–258, DOI: 10.1002/kin.21154.

(18) Class, C. A.; Vasiliou, A. K.; Kida, Y.; Timko, M. T.; Green, W. H. Detailed kinetic model for hexyl sulfide pyrolysis and its desulfurization by supercritical water. *Phys. Chem. Chem. Phys.* **2019**, *21*, 10311–10324, DOI: 10.1039/C9CP00234K.

(19) Slakman, B. L.; Simka, H.; Reddy, H.; West, R. H. Extending Reaction Mechanism Generator to Silicon Hydride Chemistry. *Ind. Eng. Chem. Res.* **2016**, *55*, 12507–12515, DOI: 10.1021/acs.iecr.6b02402.

(20) Farina, D. S.; Sirumalla, S. K.; Mazeau, E. J.; West, R. H. Extensive High-Accuracy Thermochemistry and Group Additivity Values for Halocarbon Combustion Modeling. *Ind. Eng. Chem. Res.* **2021**, DOI: 10.1021/acs.iecr.1c03076.

(21) Cobos, C. J.; Croce, A. E.; Luther, K.; Sölter, L.; Tellbach, E.; Troe, J. Experimental

and modeling study of the Reaction $C_2F_4\,(^+\mathrm{M}) \longleftrightarrow CF_2 + CF_2\,(^+\mathrm{M})$. *J. Phys. Chem. A* **2013**, *117*, 11420–11429, DOI: 10.1021/jp408363s.

(22) Gómez, N. D.; Codnia, J.; Azcárate, M. L.; Cobos, C. J. Quantum chemical and kinetic study of the CCl2 self-recombination reaction. *Computational and Theoretical Chemistry* **2017**, *1121*, 1–10, DOI: 10.1016/j.comptc.2017.10.004.

(23) Srinivasan, N. K.; Su, M.-C.; Michael, J. V.; Jasper, A. W.; Klippenstein, S. J.; Harding, L. B. Thermal Decomposition of CF_3 and the Reaction of $CF_2 + OH \longrightarrow CF_2O + H$. *J. Phys. Chem. A* **2008**, *112*, 31–37, DOI: 10.1021/jp076344u.

(24) Linteris, G.; Babushok, V. Laminar burning velocity predictions for C1 and C2 hydrofluorocarbon refrigerants with air. *J. Fluor. Chem.* **2020**, *230*, DOI: 10.1016/j.jfluchem.2019.05.002.

(25) Mathieu, O.; Keesee, C.; Gregoire, C.; Petersen, E. L. Experimental and chemical kinetics study of the effects of halon 1211 (CF_2BrCl) on the laminar flame speed and ignition of light hydrocarbons. *Phys. Chem. A* **2015**, *119*, 7611–7626, DOI: 10.1021/acs.jpca.5b00959.

(26) Needham, C. D.; Westmoreland, P. R. Combustion and flammability chemistry for the refrigerant HFO-1234yf (2,3,3,3-tetrafluoropropene). *Combust. Flame* **2017**, *184*, 176–185, DOI: 10.1016/j.combustflame.2017.06.004.

(27) Pelucchi, M.; Cavallotti, C.; Frassoldati, A.; Ranzi, E.; Glarborg, P.; Faravelli, T. Theoretical and kinetic modeling study of chloromethane (CH_3Cl) pyrolysis and oxidation. *Int. J. Chem. Kinet.* **2021**, *53*, 403–418, DOI: 10.1002/kin.21452.

(28) Kim, J.-S.; Brandt, L. M.; Heard, G. L.; Holmes, B. E. Computational study of the threshold energy for the 1,2-interchange of X and R (X, R = halogens, pseudohalogens, and monovalent hydrocarbon groups) on CH_2XCH_2R. *Can. J. Chem.* **2016**, *94*, 1038–1043, DOI: 10.1139/cjc-2016-0293.

(29) Brown, T. M.; Nestler, M. J.; Rossabi, S. M.; Heard, G. L.; Setser, D. W.; Holmes, B. E. Characterization of the 1,1-HCl Elimination Reaction of Vibrationally Excited CD_3CHFCl Molecules and Assignment of Threshold Energies for 1,1-HCl and 1,2-DCl plus 1,1-HF and 1,2-DF Elimination Reactions. *J. Phys. Chem. A* **2015**, *119*, 9441–9451, DOI: 10.1021/acs.jpca.5b06638.

(30) Brown, T. M.; Gillespie, B. R.; Rothrock, M. M.; Ranieri, A. J.; Schueneman, M. K.; Heard, G. L.; Setser, D. W.; Holmes, B. E. Unimolecular HBr and HF Elimination Reactions of Vibrationally Excited $C_2H_5CH_2Br$ and C_2D_5CHFBr: Identification of the 1,1-HBr Elimination Reaction from C_2D_5CHFBr and Search for the $C_2D_5(F)C$:HBr Adduct. *J. Phys. Chem. A* **2019**, *123*, 8776–8786, DOI: 10.1021/acs.jpca.9b07029.

(31) Smith, C. A.; Gillespie, B. R.; Heard, G. L.; Setser, D. W.; Holmes, B. E. The Unimolecular Reactions of CF_3CHF_2 Studied by Chemical Activation: Assignment of Rate Constants and Threshold Energies to the 1,2-H Atom Transfer, 1,1-HF and 1,2-HF Elimination Reactions, and the Dependence of Threshold Energies on the Number of F-Atom Substituents in the Fluoroethane Molecules. *J. Phys. Chem. A* **2017**, *121*, 8746–8756, DOI: 10.1021/acs.jpca.7b06769.

(32) Yu, H.; Mackie, J. C.; Kennedy, E. M.; Dlugogorski, B. Z. Experimental and Quantum Chemical Study of the Reaction $CF_2 + CH_3 \longleftrightarrow CF_2CH_3 \longrightarrow CH_2CF_2 + H$: A Key Mechanism in the Reaction between Methane and Fluorocarbons. *Ind. Eng. Chem. Res.* **2006**, *45*, 3758–3762, DOI: 10.1021/ie060221z.

(33) Blowers, P.; Masel, R. Engineering approximations for activation energies in hydrogen transfer reactions. *AIChE J.* **2000**, *46*, 2041 – 2052, DOI: 10.1002/aic.690461015.

(34) Bhoorasingh, P. L.; Slakman, B. L.; Seyedzadeh Khanshan, F.; Cain, J. Y.; West, R. H. Automated Transition State Theory Calculations for High-Throughput Kinetics. *J. Phys. Chem. A* **2017**, *121*, 6896–6904, DOI: 10.1021/acs.jpca.7b07361.

(35) Harms, N.; Underkoffler, C.; West, R. Advances in automated transition state theory calculations: improvements on the AutoTST framework. *ChemRxiv Preprint* **2020**, DOI: 10.26434/chemrxiv.13277870.

(36) Landrum, G. RDKit: Open-source cheminformatics. http://www.rdkit.org.

(37) Aradi, B.; Hourahine, B. dftbplus/dftbplus [DFTB+]: Release 17.1. 2017.

(38) Kubař, T.; Bodrog, Z.; Gaus, M.; Köhler, C.; Aradi, B.; Frauenheim, T.; Elstner, M. Parametrization of the SCC-DFTB method for halogens. *J. Chem. Theory Comput* **2013**, *9*, 2939–2949, DOI: 10.1021/ct4001922.

(39) Larsen, A. H.; others The atomic simulation environment—a Python library for working with atoms. *J. Condens. Matter Phys.* **2017**, *29*, 273002, DOI: 10.1088/1361-648X/aa680e.

(40) Frisch, M. J.; others Gaussian 16 Revision B.01. 2016; Gaussian Inc. Wallingford CT.

(41) Grimme, S.; Antony, J.; Ehrlich, S.; Krieg, H. A consistent and accurate ab initio parametrization of density functional dispersion correction (DFT-D) for the 94 elements H-Pu. *Chem. Phys.* **2010**, *132*, DOI: 10.1063/1.3382344.

(42) Papajak, E.; Zheng, J.; Xu, X.; Leverentz, H. R.; Truhlar, D. G. Perspectives on basis sets beautiful: Seasonal plantings of diffuse basis functions. *J. Chem. Theory Comput.* **2011**, *7*, 3027–3034, DOI: 10.1021/ct200106a.

(43) Mardirossian, N.; Head-Gordon, M. Thirty years of density functional theory in computational chemistry: An overview and extensive assessment of 200 density functionals. *Mol. Phys.* **2017**, *115*, 2315–2372, DOI: 10.1080/00268976.2017.1333644.

(44) Kozuch, S.; Martin, J. M. Halogen bonds: Benchmarks and theoretical analysis. *J. Chem. Theory Comput.* **2013**, *9*, 1918–1931, DOI: 10.1021/ct301064t.

(45) Forni, A.; Pieraccini, S.; Rendine, S.; Sironi, M. Halogen bonds with benzene: An assessment of DFT functionals. *Comp Chem* **2014**, *35*, 386–394, DOI: 10.1002/jcc.23507.

(46) Neese, F. The ORCA program system. *Wiley Interdiscip. Rev.: Comput. Mol. Sci.* **2012**, *2*, 73–78, DOI: 10.1002/wcms.81.

(47) Arkane: Automated Reaction Kinetics and Network Exploration. https://reactionmechanismgenerator.github.io/RMG-Py/users/arkane/, Accessed: 2019–01-29.

(48) Smith, G. P.; Tao, Y.; Wang, H. Foundational Fuel Chemistry Model Version 1.0. 2016; http://nanoenergy.stanford.edu/ffcm1.

(49) Devotta, S.; Pendyala, V. R. Modified Joback group contribution method for normal boiling point of aliphatic halogenated compounds. *Industrial & Engineering Chemistry Research* **1992**, *31*, 2042–2046, DOI: 10.1021/ie00008a029.

(50) Farina, D., Jr. Automating Reaction Mechanism Generation of Halocarbon Combustion and Electrochemical Catalysis. Ph.D. thesis, Northeastern University, 2022, DOI: 10.17760/D20467257.

(51) Goodwin, D. G.; Moffat, H. K.; Speth, R. L. Cantera: An Object-oriented Software Toolkit for Chemical Kinetics, Thermodynamics, and Transport Processes. http://www.cantera.org, 2017; Version 2.3.0.